



Combining mass spectrometry, i^2 PEPICO, and FTIR spectroscopy: Comprehensive speciation in DMM/NO oxidation

Steffen Schmitt^{a,*}, Nina Gaiser^a, Hao Zhang^b, Alessandro Stagni^c, Jasmin Bachmann^a, Patrick Oßwald^a, Katharina Kohse-Höinghaus^d, Markus Köhler^a

^a Institute of Combustion Technology, German Aerospace Center, Stuttgart 70569, Germany

^b State Key Laboratory of Clean Energy Utilization, Zhejiang University, Hangzhou 310027, China

^c Department of Chemistry, Materials, and Chemical Engineering "G. Natta", Politecnico di Milano, Milano 20133, Italy

^d Department of Chemistry, Bielefeld University, Bielefeld 33615, Germany

ARTICLE INFO

Keywords:

Oxymethylene ethers
NO
Dimethoxy methane
Molecular-Beam mass spectrometry
FTIR spectroscopy
 i^2 PEPICO
Plug-Flow reactor

ABSTRACT

Oxymethylene ethers (OMEs) are potential alternative fuels that can be produced in a sustainable way based on CO₂ and electricity. Additionally, they exhibit low tendencies to emit NO_x or soot during practical combustion. Dimethoxy methane (DMM, CH₃OCH₂OCH₃) has received increasing attention as the smallest OME with a O-CH₂-O moiety. In the face of a possible application in exhaust gas recirculation (EGR) scenarios, understanding the influence of NO_x on DMM oxidation is of importance. In this work, eleven mixtures of DMM/NO/O₂/Ar were investigated in an atmospheric laminar flow reactor employing an extensive set of diagnostics. Molecular-beam mass spectrometry (MBMS), Fourier-transform infrared (FTIR) spectroscopy, NO_x chemiluminescence detection, and double imaging photoelectron photoion coincidence (i^2 PEPICO) spectroscopy were combined to obtain a reliable speciation. All in all, species concentrations from different instruments showed a good agreement and one technique could counterbalance the physical limitations of another technique in many cases. In this manner, accurate mole fraction profiles of intermediates like e.g. CH₄, C₂H₄, NO₂, and methyl formate (C₂H₄O₂) were gained. Based on i^2 PEPICO results, nitromethane (CH₃NO₂) and *trans*-HONO could additionally be identified as crucial intermediates in the NO-assisted oxidation of DMM. The present data set therefore provides an excellent basis to enhance future model development.

1. Introduction

In the context of the concerted global effort to mitigate greenhouse gas emissions, oxymethylene ethers (OMEs, CH₃O(CH₂O)_nCH₃) are gaining increased attention as promising alternative fuel. Synthesized from sustainable resources, e.g. CO₂ and electric power (E-fuels), their combustion emissions feature low soot / NO_x [1–4]. While significant recent work has been performed regarding the combustion and oxidation chemistry of OMEs family fuels (e.g., $n = 0–5$) [4–7], the chemical interaction between OMEs and NO_x, an enduring focus of combustion research, has been rarely explored in both experimental and modeling aspects [7–10]. The comparatively unsatisfactory model predictions observed in recent studies on dimethyl ether (DME, CH₃OCH₃, as OME₀) oxidation with NO addition clearly underscored the complexity of the interaction between the OMEs fuel species and NO_x [7,11]. While DME is established as an alternative fuel, DMM might be considered mainly in

fuel blends. However, its additional -CH₂O moiety, which is a representative feature also in the larger OME molecules discussed as e-fuels, adds complexity in the reaction chemistry and consequent combustion behavior regarding ignition, low-temperature pathways and pollutant formation.

Comprehensive information on the involved reactive species is essential for understanding a combustion / oxidation process, involving various combustion diagnostics such as noninvasive laser and optical techniques, probe-sampling techniques with mass spectrometry (MS), Fourier-transform infrared (FTIR) spectroscopy, and gas chromatography (GC) etc. [2]. Even powerful and universal methods such as molecular-beam mass spectrometry (MBMS) often fall short of providing a complete quantitative characterization via a single analysis method [12]. For instance, in our recent efforts to elucidate the species pool of DME and dimethoxy methane (DMM, CH₃OCH₂OCH₃, OME₁) oxidation with NO addition, utilizing laboratory-based electron ionization

* Corresponding author.

E-mail address: steffen.schmitt@dlr.de (S. Schmitt).

<https://doi.org/10.1016/j.proci.2024.105365>

Received 3 December 2023; Accepted 12 June 2024

Available online 28 June 2024

1540-7489/© 2024 The Combustion Institute. Published by Elsevier Inc. All rights are reserved, including those for text and data mining, AI training, and similar technologies.

(EI)-MBMS revealed challenges in reliably identifying and/or quantifying key N-species such as NO_2 , HNO_2 , CH_3NO_2 and/or even NO , due to mass overlaps and potential intermediates' fragmentation [7,11]. Additionally, the high uncertainty in quantifying intermediates or radicals, typically up to a factor of 2–4, complicates model validation [11–13]. The modest energy resolution of the ionizing electron beam (typically $E/\Delta E < 20$) in EI-MBMS does not allow for an isomeric determination.

In this study, we selected DMM as the first OME with an $\text{O-CH}_2\text{-O}$ moiety to comprehensively unravel the chemical composition of OMEs oxidation in the presence of NO . Eleven DMM/ NO gas mixtures were investigated with varying equivalence ratios (0.8, 1.2, 2.0) and NO additions (0, 200, 500, 900 ppm) in an atmospheric laminar flow reactor (PFR). Different state-of-the-art techniques, including EI-MBMS, FTIR spectroscopy, chemiluminescence NO_x -sensor, and double imaging photoelectron photoion coincidence (i^2 PEPICO) spectroscopy, were combined to provide a comprehensive and isomer-resolved new speciation dataset. These reliable data are expected to significantly contribute to a better understanding of OMEs/ NO interactions. Although it can serve as a basis for future model development, it is beyond the scope of this study to develop a kinetic mechanism.

2. Experimental setup

The majority of experiments were carried out at DLR's atmospheric laminar flow reactor (DLR reactor: 1497 mm length, 40 mm inner diameter) originally described in [14] and used for several works already also reporting oxidation experiments of neat OMEs [5,15]. During an experiment, reactant gasses flow continuously into the reactor controlled by Coriolis flow meters (Bronkhorst). DMM (99%, Sigma-Aldrich) is evaporated first at 373 K by a commercial vaporizer (Bronkhorst CEM) and fed into a pre-heating line (373 K) to avoid condensation. Measurements were started at a reactor temperature of 1170 K. Then the reactor temperature was decreased by 200 K per hour until no reaction was observed (~ 700 K).

The complete dataset for all conditions (see Table 1) is provided with the electronic supplement including an overview of applied techniques for the respective species mole fraction profiles as well as empiric reactor temperature profiles based on [5].

2.1. Molecular-beam mass spectrometry

Sample gasses were continuously guided from the reactor exit (~ 980 mbar) through a two-stage expansion (1st stage $\sim 10^{-4}$ mbar, 2nd stage $\sim 10^{-5}$ mbar) into an electron impact reflectron time-of-flight (TOF) mass spectrometer ($\sim 10^{-7}$ mbar) with a nominal electron energy of 13.5 eV.

Species signals were quantified by using argon as an inert reference species and calibration factors either derived from an elemental balance (major species) or direct calibration (typical intermediates) approach.

Table 1
Experimental conditions investigated in this work.

Gas mixture	Inlet mole fractions				φ	Total flow rate / slm	Residence time τ
	DMM	Ar	NO / ppm	O_2			
DMM_0.8_200NO	0.00167	0.9898	200	0.00833	0.8	10	$\tau = \frac{2520\text{s}\cdot\text{K}}{T} + 1.7\text{s}$
DMM_0.8_900NO	0.00167	0.9891	900	0.00833	0.8	10	
DMM_1.2_0NO	0.00231	0.9900	0	0.00769	1.2	10	
DMM_1.2_200NO	0.00231	0.9898	200	0.00769	1.2	10	
DMM_1.2_500NO	0.00231	0.9895	500	0.00769	1.2	10	
DMM_1.2_900NO	0.00231	0.9891	900	0.00769	1.2	10	
DMM_2.0_0NO	0.00333	0.9900	0	0.00667	2.0	10	
DMM_2.0_200NO	0.00333	0.9898	200	0.00667	2.0	10	
DMM_2.0_500NO	0.00333	0.9895	500	0.00667	2.0	10	
DMM_2.0_900NO	0.00333	0.9891	900	0.00667	2.0	10	
DMM_0.8_900NO_93Ar	0.01167	0.9291	900	0.05833	0.8	3.025	4.1 s at 833 K

Since EI-MBMS is a commonly employed technique in combustion science, the reader is referred to previous works for a more detailed description of its principles and data evaluation [16–18]. Comprehensive discussion on experimental errors are available in the literature as well [12,13,17,18]. To summarize, typical uncertainties are less than $\pm 20\%$ for species quantified by direct calibration or elemental balance and up to a factor of 2–4 for species where the relative ionization cross section (RICS) [16] approach is used for quantification. All species-specific calibration methods and resulting uncertainties are given in Table S1 in SM1.

2.2. FTIR spectroscopy

MBMS techniques based on electron ionization do not enable isomer assignment and sometimes lead to challenging data interpretation due to overlapping species and fragmentation processes. Therefore, a FTIR spectrometer (Matrix-MG5, Bruker Optics) was adapted to the DLR reactor with a heat-resistant, austenitic stainless steel (material number: 1.4841) sample head positioned near the quartz nozzle of the MBMS setup. The sample gasses were then guided through a tube (diameter 6 mm, ~ 100 cm length) into a gas cell heated at 453 K. FTIR spectra were measured at a resolution of 0.5 cm^{-1} and 10 spectra were summed up for one measurement point.

Species quantification was performed with the OPUS GA software package and commercial FTIR spectra database by Bruker Optics. Evaluated spectral ranges were optimized for each species to reduce the effect of overlapping absorbances. The selected spectral range was then fitted with the algorithm employed in OPUS GA while also considering further contributing species and the background signal. Fits below a minimal correlation limit were discarded and the corresponding species' concentration was set to zero to avoid false assignment of spectral absorbances.

Although the accuracy of the instrument is considered to be ± 1 ppm for single species in an inert dilution gas, it is to be expected that the complexity of a combustion-generated and temperature-dependent mixture leads to a higher uncertainty. Therefore, the identical uncertainty to directly calibrated EI-MBMS species ($\pm 20\%$) is assumed and discussed further in Section 3, where the experimental results are presented in comparison.

2.3. NO_x -sensor

A NO_x -sensor based on chemiluminescence of ozone-activated NO_2^* (CLD700, Ecophysics) is adapted to the reactor by adding a tube from the FTIR spectrometers' exhaust gas line. The internal pump of the NO_x -sensor ensures a constant flow rate of 1.2 slm through both FTIR spectrometer and NO_x -sensor. The CLD700 sensor is capable of quantifying NO and NO_x simultaneously at a measurement rate of 1 Hz. NO_2 is automatically calculated from the difference of NO_x and NO .

2.4. i^2 PEPICO

Measurements using i^2 PEPICO spectroscopy were performed to further identify crucial isomers at the VUV (X04DB) beamline of the Swiss Light Source (SLS). To obtain clear signals for intermediate species with a favorable signal-to-noise ratio, the argon dilution was decreased to 93% to increase the respective intermediate species concentrations. Another flow reactor (1000 mm length, 22 mm inner diameter) called PIRO [5] was used for these experiments, but the total flow rate was adapted accordingly to 3.025 slm to ensure similar residence time behavior compared to the experiments conducted in the DLR reactor (see Table 1).

Please note that it was not possible to investigate a whole temperature ramp due to limited beamtime. Therefore, all i^2 PEPICO experiments were performed at only one constant reactor temperature T of 833 K, which equals a gas flow temperature of 780 K. This temperature was chosen, since it corresponds to a maximum signal intensity at a mass-to-charge ratio $m/z = 61$ (CH_3NO_2). The photon energy was scanned from 9.95 to 11.7 eV with a step size of 0.025 eV. At each photon energy, photoions and photoelectrons were detected coincidentally. A detailed description of this technique can be found in [19–21]. Mass-selected threshold photoelectron spectra (ms-TPES) were then extracted from the raw signals following a well-established procedure [21,22]. Species information are gained by comparing the measured spectra to pure compound reference spectra and the corresponding ionization threshold.

3. Results

This section presents the experimental results and the insight gained on the interaction between DMM and NO based on the combination of EI-MBMS, FTIR, NO_x -sensor, and i^2 PEPICO techniques. First, the general reactivity will be discussed (Section 3.1) followed by a deeper analysis of

intermediate species quantified with different techniques and instruments (Section 3.2). Then, ms-TPES gained from i^2 PEPICO experiments are used to identify crucial intermediates in the NO-assisted oxidation of DMM (Section 3.3). As concluding part, the results are examined from a kinetic perspective and suggestions regarding model development are presented (Section 3.4).

3.1. General reactivity

Fig. 1 shows the mole fraction profiles of DMM as a representative reactant and H_2O as a product, respectively. Corresponding data for O_2 and CO_2 is shown in Fig. S1 in SM1. Please note that the data in Fig. 1(a) corresponds to previous work [5], but is shown here for a more complete picture. In general, the reactivity is increased by NO addition as evident from the fuel consumption at lower temperatures with increasing NO amount (200 to 900 ppm), although the influence is not strong (consider also the estimated temperature uncertainty of about ± 5 K [5]). Also, the influence of NO depends only weakly on the equivalence ratio for the investigated cases. Only selected conditions are thus presented in the following discussion and the reader is referred to SM2 for the complete data set.

For all investigated cases, agreement of DMM and CO_2 (Fig. S1 in SM1) mole fractions measured by EI-MBMS and FTIR is nearly perfect. Regarding the different physical principles of both methods, the excellent quantitative agreement underlines the power of the present approach. Also, this finding provides confidence that the adaption of the FTIR spectrometer to the DLR reactor is successful and that sampling effects do not play a significant role in the current setup. Existing response time differences between the FTIR gas cell and the mass spectrometer are negligible compared to the applied temperature ramp as can be seen from the absence of any temperature shift between EI-MBMS and FTIR results.

H_2O mole fraction profiles in Fig. 1 agree within the respective

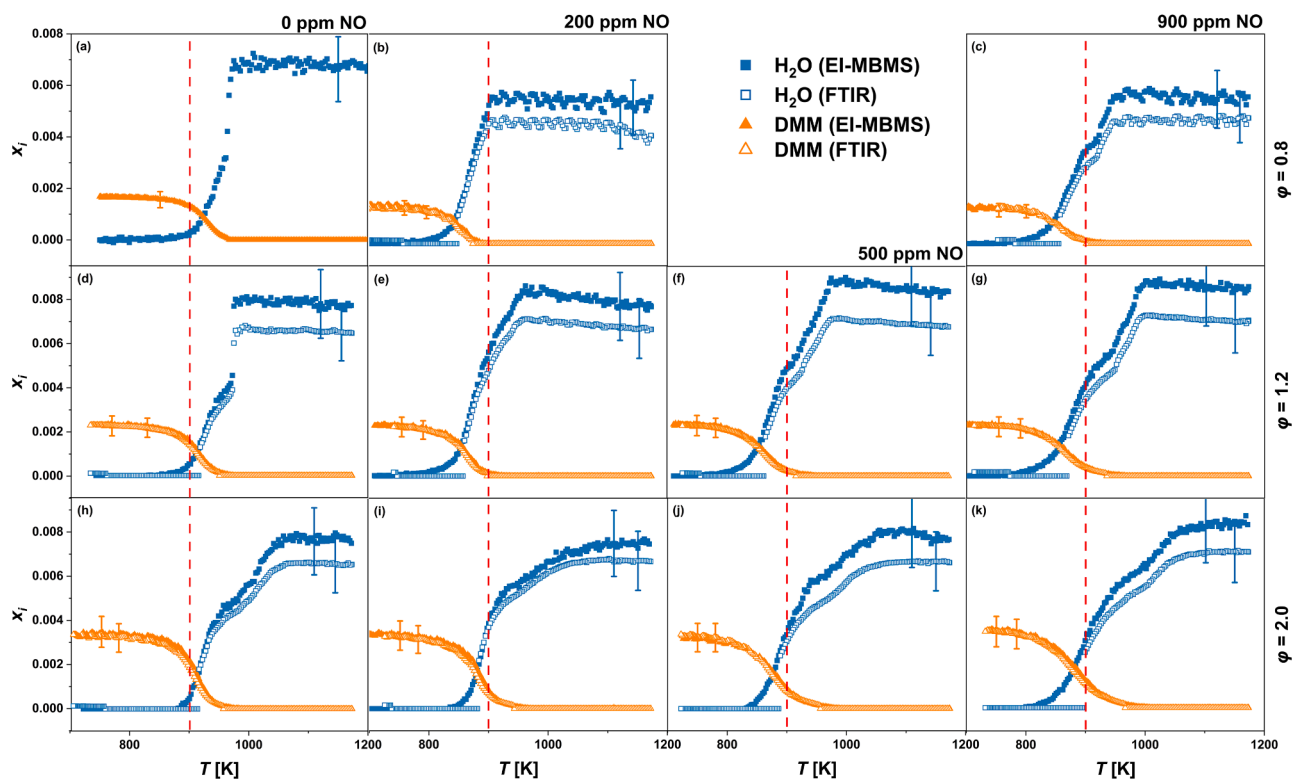


Fig. 1. Mole fraction profiles of DMM and water (H_2O) quantified by both EI-MBMS (filled symbols) and FTIR (open symbols). (a) Data by Gaiser et al. [5], (b)–(k) this work. The estimated uncertainty of $\pm 20\%$ is indicated at only one point for clarity and vertical dashed lines were added to highlight the different onsets. Note the overlap of the results with EI-MBMS and FTIR for the DMM traces.

experimental uncertainties but with larger discrepancy than for DMM. These differences could result from water in the background FTIR spectrum, an assumption supported by the later onset of the FTIR H₂O mole fraction profiles. Please note that the FTIR H₂O background depends not only on H₂O in the gas cell but also within the optics of the spectrometer. However, the effect of H₂O in the optics of the spectrometer is expected to be small, since a molecular sieve is used to minimize H₂O contributions. Since one aim of this study is to evaluate and use the potential of combining FTIR and EI-MBMS, it was not attempted, although possible, to post-calibrate H₂O (FTIR) with the elemental balance approach used for the major species in EI-MBMS data.

The H₂O mole fraction profiles of both instruments indicate a second ignition step, evident from the slight delay in the increase of H₂O between 900 and 1000 K. This could originate from the change from low- to intermediate-temperature oxidation, which is less pronounced for DMM than for dimethyl ether (DME) [7].

Previous studies have obtained contrasting results regarding NO consumption. While Zhang et al. [7] observed that NO was not completely consumed in EI-MBMS experiments at 93% argon dilution, later results by *i*²PEPICO [11] indicated a complete NO consumption in DME/NO experiments. An accurate NO quantification via EI-MBMS is challenging since significant overlap with C¹⁸O and CH₂O influences the NO signal; also, fragmentation from e.g., NO₂ and HONO (see SM1 of [11]) possibly contributes to the NO signal at *m/z* = 30. The selected combination of methods can resolve these issues that could be causing the deviations of the NO (EI-MBMS) profile in Fig. 2 from the other two curves and the higher scatter of the data.

The present experiments indicate that NO is not consumed completely (see Fig. 2), confirmed by all three instruments that quantify NO following different physical principles. Especially the NO_x-sensor and FTIR data show excellent agreement. For the high fuel/NO ratio in the DMM_0.8_900NO_93Ar case, the absence of NO in the reacting regime could be proven by *i*²PEPICO spectroscopy (see Fig. S2 in SM1) in agreement with Pelucchi et al. [11]. It can thus be concluded that the fuel/NO ratio is the key parameter that governs whether NO is consumed completely.

3.2. Intermediate species

After summarizing the general reactivity of DMM/O₂/NO/Ar mixtures, the reaction properties are further analyzed by discussing selected intermediate species as exemplarily shown in Fig. 3 for the DMM_2.0_500NO case. Methane (CH₄, Fig. 3(a)) can be considered as a

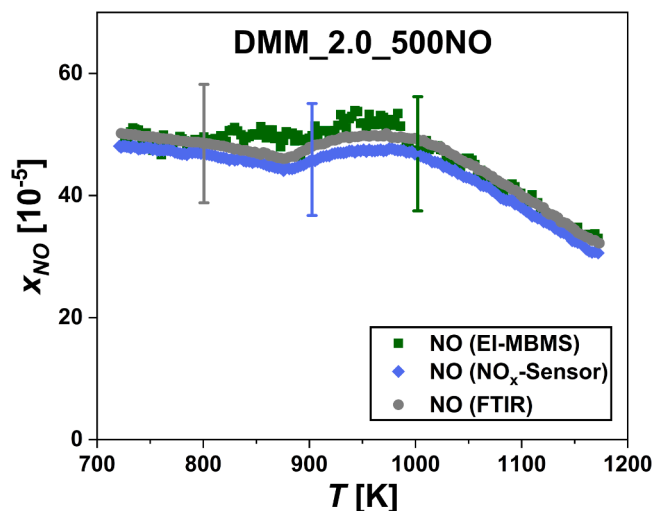


Fig. 2. NO mole fractions for the DMM_2.0_500NO case obtained by EI-MBMS, NO_x sensor, and FTIR. The estimated uncertainty of ±20% is indicated at only one point for clarity.

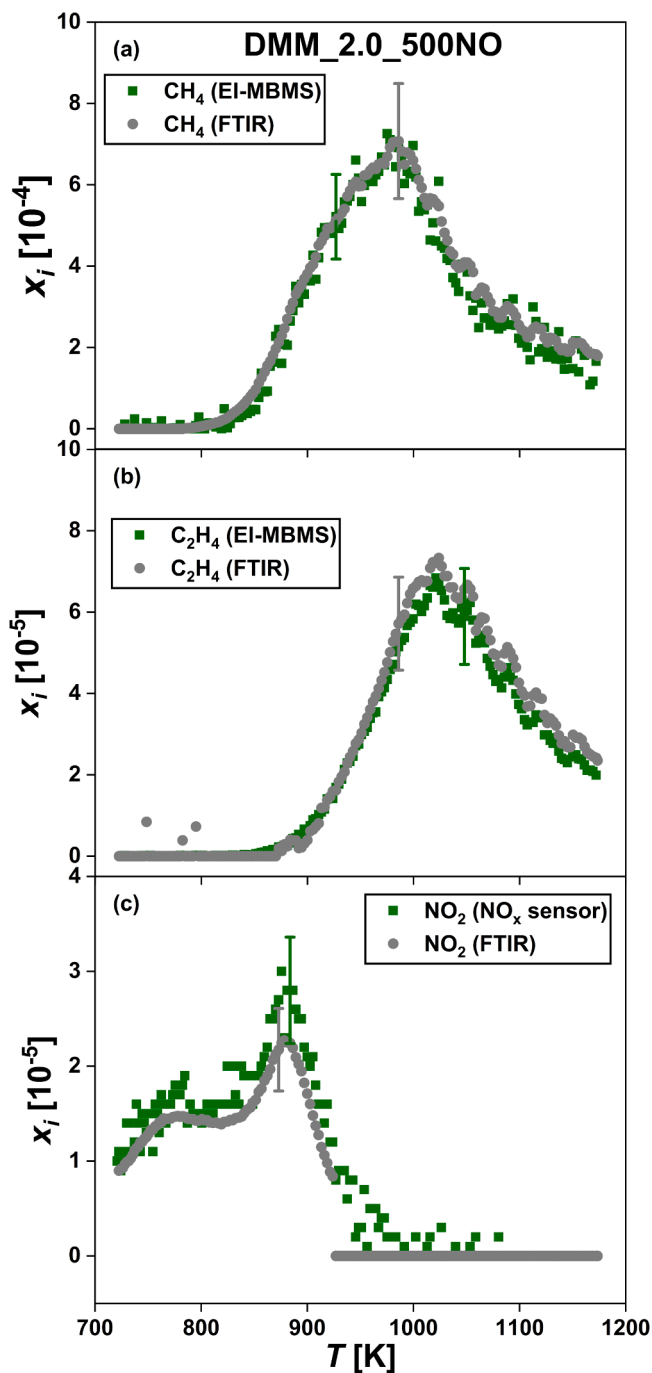


Fig. 3. Mole fraction profiles of CH₄ (a), C₂H₄ (b), and NO₂ (c) obtained by different instruments for the DMM_2.0_500NO case. The estimated uncertainty of ±20% is indicated at only one point for clarity.

rather stable proxy for the highly reactive methyl (CH₃) radicals that are formed in many of DMM's initial decomposition steps.

Ethene (C₂H₄, Fig. 3(b)) is built up from precursor reactions. Its mole fraction is approximately one order of magnitude larger in the fuel-rich mixtures than in the fuel-lean ones. Once again, EI-MBMS and FTIR results are almost identical indicating that the estimated uncertainty could be lowered by combining both instruments where neither technique faces a specific challenge.

NO₂ mole fraction profiles (Fig. 3(c)) show two peaks for both NO_x-sensor and FTIR spectrometer. Since the first peak corresponds to a temperature (~750 K) where DMM is not consumed yet, this indicates an interconversion from NO that does not influence the DMM reactivity,

in contrast to the second peak (~ 850 K) that coincides with the reaction zone of DMM. However, rather small amounts of NO_2 were detected that correspond to only about 4% of the NO added. NO_2 could not be quantified by EI-MBMS due its significant fragmentation tendency towards NO and overlaps with fragments of DMM.

The good agreement between EI-MBMS and FTIR described before implies that calibration of the MBMS signals by using the corresponding FTIR concentrations is possible. This has been done for methyl formate in Fig. 4, based on the methyl formate concentration obtained by FTIR for the DMM_2.0_900NO case. Nonetheless, this approach is only valid, if all present isomers are quantified by FTIR spectroscopy and raw signal profiles have identical shapes.

Limitations of the FTIR technique were observed, when species show quite similar absorbances or when high-resolution reference spectra are unavailable for the investigated conditions (453 K and Ar dilution). An example of the first issue is DME which could not be quantified by the FTIR spectrometer due to its similarity to DMM, although mole fraction profiles could be obtained for $\text{C}_2\text{H}_6\text{O}$ by EI-MBMS (see Fig. S2 in SM1).

Trans-HONO and nitromethane (CH_3NO_2), previously identified as crucial intermediates in the interaction between DME and NO [11], could both not be detected by FTIR spectroscopy due to lacking high-resolution reference spectra. Also, EI-MBMS experiments are unable to prove the presence of these species due its lack in isomer selectivity, and high fragmentation tendency. i^2 PEPICO spectroscopy is used to investigate whether these species also play a crucial role for the DMM/NO reaction network and to resolve molecular structures of the respective sum formula obtained by EI-MBMS. The corresponding results are discussed in the following section.

3.3. Crucial isomers analyzed by i^2 PEPICO

The molecular structure of intermediates can be determined by comparing the obtained ms-TPES with reference PES as shown in Fig. 5. The ms-TPES corresponding to $m/z = 60$ agrees well with the reference PES of methyl formate by Nunes et al. [23]. Since no additional signals were detected, it can be concluded that methyl formate is the only $\text{C}_2\text{H}_4\text{O}_2$ isomer present in the experiments, supporting the approach to calibrate EI-MBMS based on the FTIR-derived concentrations (see Fig. 4). Formaldehyde and methanol were identified as additional oxygenated intermediates (see Fig. S3 and S4 in SM1).

At $m/z = 61$, the measured ms-TPES corresponds mainly to the reference spectrum of nitromethane by Hoener et al. [24]. A small peak is present at around 10.5 eV which might indicate minor amounts of

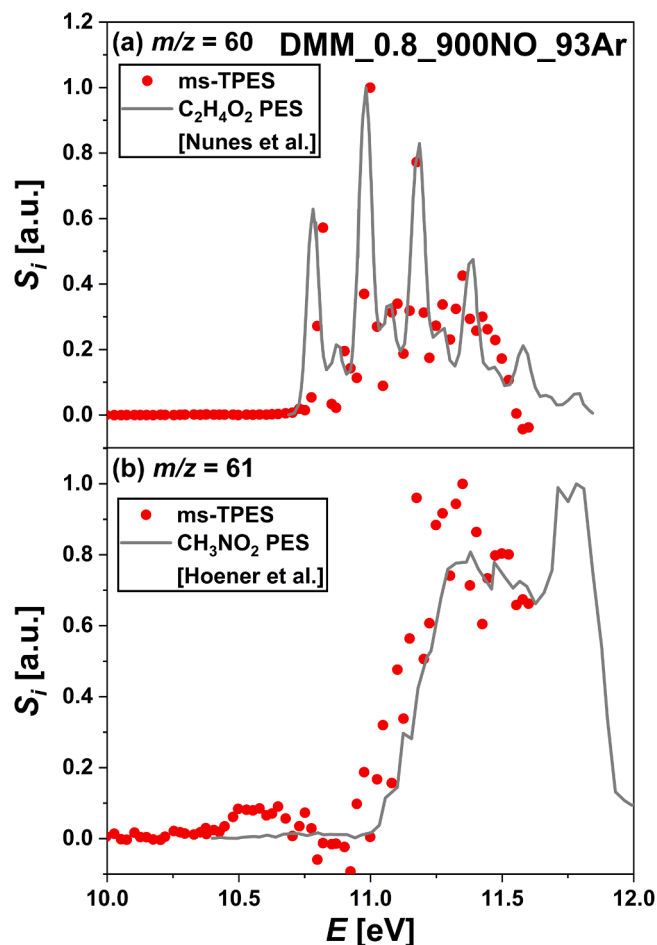


Fig. 5. Mass-selected TPES for $m/z = 60$ (a) and 61 (b) with literature PES for methyl formate ($\text{C}_2\text{H}_4\text{O}_2$) [23] and nitromethane (CH_3NO_2) [24].

methyl nitrite (CH_3ONO , IP: 10.44 eV [25]), but to the best of the authors' knowledge, there is no reference spectrum with a sufficient spectral resolution available of CH_3ONO in the literature. Additionally, the presence of *trans*-HONO could be concluded by the corresponding ms-TPES at $m/z = 47$ (see Fig. S5 in SM1). These species have been identified as most important interaction species in a previous study in DME/NO experiments [11], which leads to the assumption that the species pool necessary to describe higher OMEs/ NO_x interactions is similar.

3.4. Key aspects of DMM/NO kinetics

Although the literature offers several examples of detailed kinetic mechanisms of DMM pyrolysis and oxidation [10,26–29], to the authors knowledge there is no comprehensive modeling study of the interaction between DMM and NO/ NO_2 published yet. As a first approach, considering previous kinetic studies on DME/NO oxidation [10,11,30], it is reasonable to assume a comparable mechanistic description of the system. In qualitative terms, this can be schematized as in Fig. 6. The complex interplay between NO and hydrocarbon chemistry can be schematized as occurring at two different levels: (i) interaction with C_1 fragments, and (ii) direct reaction with DMM and its reaction products. The theoretical understanding of NO_x/C_1 systems is now well-established [31]. A sensitizing effect occurs through the formation of NO_2 in the temperature region where DMM is consumed (through the chain propagation reaction $\text{NO} + \text{HO}_2 \rightarrow \text{NO}_2 + \text{OH}$). As a consequence, the methoxy radical is formed ($\text{CH}_3 + \text{NO}_2 \rightarrow \text{CH}_3\text{O} + \text{NO}$) and subsequently decomposed to CH_2O and H, enhancing the reactivity. This

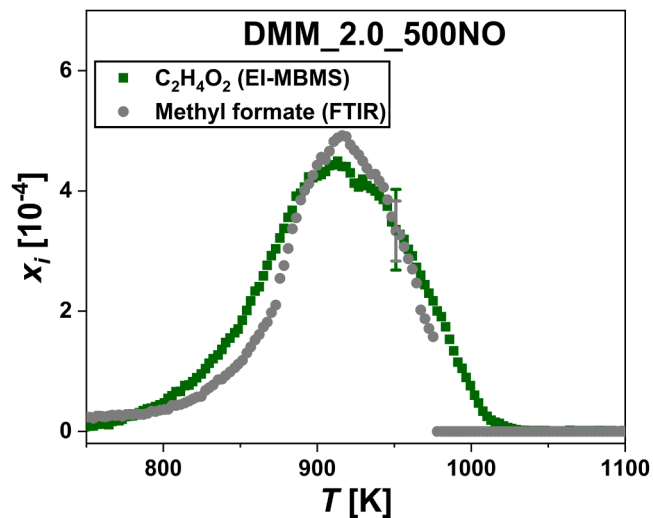


Fig. 4. Mole fraction profile of methyl formate for the DMM_2.0_500NO case. The estimated uncertainty of $\pm 20\%$ is indicated at only one point for clarity.

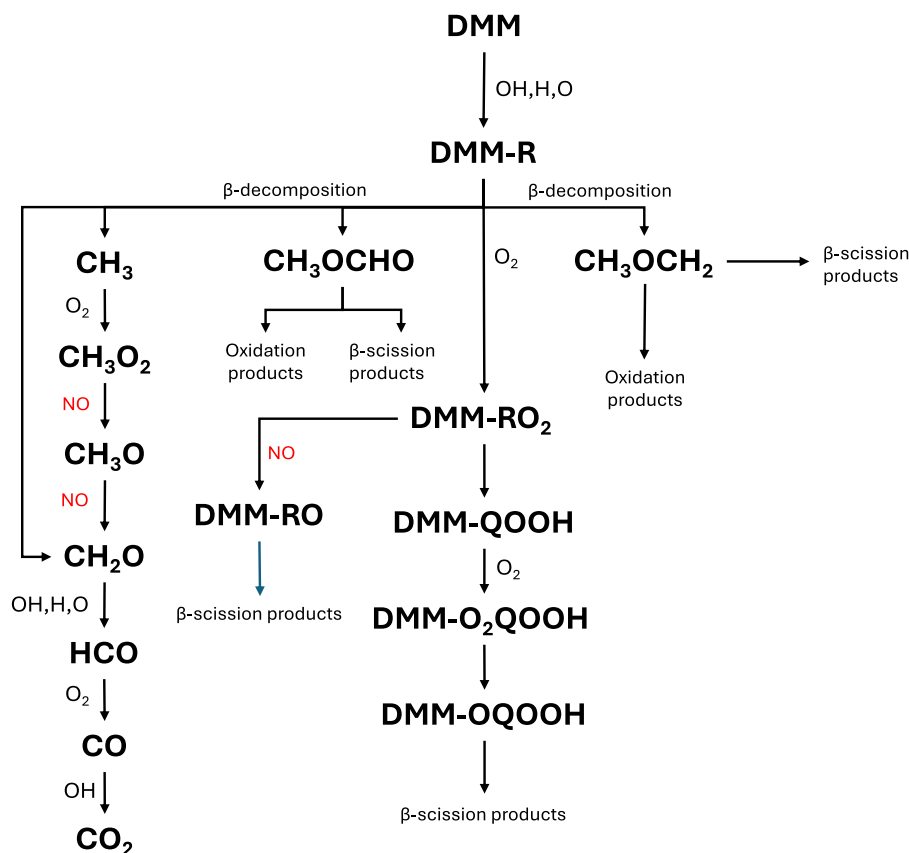


Fig. 6. Flux diagram for DMM oxidation, highlighting the two-level interaction between DMM and NO.

effect is counteracted by the inhibiting one caused by the formation of nitromethane (CH_3NO_2) via radical recombination.

Nevertheless, the coupling between NO and higher intermediates is mostly unexplored from a theoretical point of view, and mostly relies on the analogy with smaller molecules and rate rules. At such temperatures, NO intercepts the low-temperature reaction path by reacting with the DMM peroxide and provides the more reactive alkoxy radical isomers: $\text{DMM-RO}_2 + \text{NO} \rightarrow \text{DMM-RO} + \text{NO}_2$. This paves the way to alkoxy fragmentation, and according to the formed isomer, the formation of either the methoxy radical ($\text{CH}_3\text{OCH}_2\text{O}$) or the methyl formate radical (CH_2OCHO), which was previously discussed in Section 3.2. Pelucchi et al. [11] already identified methyl formate as a key species in the chemistry of DME/NO interaction, which has been also studied in recent works due to its role as an intermediate in DME/DMM combustion [32, 33]. Within DMM oxidation, methyl formate is mostly formed from the decomposition of $\text{CH}_3\text{OCH}_2\text{O}$ itself into $\text{CH}_3\text{OCHO} + \text{H}$. Such a step is strongly pressure-dependent, with large disagreements in literature about the related rates [34].

Once methyl formate is obtained, H-abstraction by NO_2 becomes possible from both methyl formate [35] and DMM itself, triggering reactivity ($\text{DMM} + \text{NO}_2 \rightarrow \text{DMM-R} + \text{HONO}/\text{HNO}_2$ and $\text{CH}_3\text{OCHO} + \text{NO}_2 \rightarrow \text{CH}_3\text{OCO} + \text{HONO}/\text{HNO}_2$, respectively). Both of them boost the reactivity, as already shown in the analysis of DME/NO system [11].

Unfortunately, to date no theoretical analysis of such rates has been done. The nearest rates available are those calculated for H-abstraction by NO_2 from DME, in reasonable agreement among the different authors [36,37].

4. Conclusion

The present work provides data sets for eleven different conditions investigating the influence of NO on DMM oxidation at low to

intermediate temperatures, including accurate quantitative species profiles. For this purpose, a unique method combination has been established by adapting two additional instruments –FTIR spectrometer and NO_x sensor– to the DLR reactor equipped with EI-MBMS. Measuring species with different techniques demonstrated a significant increase in reliability, reduced experimental uncertainties, and helped to overcome individual limitations of specific techniques.

Moreover, *trans*-HONO and CH_3NO_2 as crucial interaction species between DMM and NO chemistry were identified by i^2 PEPICO spectroscopy. This combination of accurate quantitative data and structure determination provides an excellent basis for developing a detailed state-of-the-art mechanism for the DMM/ NO_x system.

Novelty and significance statement

The work presents a unique approach that combines multiple experimental techniques coupled to a flow reactor, for species identification and quantification (i^2 PEPICO, FTIR, mass spectrometry). The aim is to enhance data quality by reducing uncertainty and compensating limitations (e.g., regarding isomer separation) of each technique alone. Such combination permits investigation of the targeted complex interaction chemistry.

The investigation is significant because chemical interactions in systems of potential replacement fuels for fossil fuels (DMM as a member of the oxymethylene ether fuel family) with exhaust gas components such as NO is relevant for EGR conditions. DMM-NO interactions were scarcely studied before, and no designated and validated DMM/NO mechanism is available yet, making the comprehensive dataset obtained here a valuable basis for model development.

Author contributions

SS performed research, analyzed data and wrote parts of the paper
 NG performed research and PEPICO data analysis
 HZ assisted in data evaluation and wrote parts of the paper
 AS provided kinetic expertise and wrote parts of the paper
 JB performed PEPICO experiments
 PO designed and performed research
 KKH designed research and supported writing the paper
 MK supervised research and supported writing the paper

Declaration of competing interest

The authors declare that they have no known competing financial interests or personal relationships that could have appeared to influence the work reported in this paper.

Acknowledgements

Experiments were performed at the VUV (X04DB) beamline of the Swiss Light Source (SLS) with the support of Patrick Hemberger and technical assistance by Torsten Methling as well as Patrick Ascher which is gratefully acknowledged. Hao Zhang is grateful for a fellowship of the Alexander von Humboldt (AvH) Foundation that supported his research in Germany. Financial support is greatly acknowledged by the DLR project NeoFuels.

Supplementary materials

Supplementary material associated with this article can be found, in the online version, at [doi:10.1016/j.proci.2024.105365](https://doi.org/10.1016/j.proci.2024.105365).

References

- [1] K. Kohse-Höinghaus, Combustion in the future: The importance of chemistry, *Proc. Combust. Inst.* 38 (2021) 1–56.
- [2] K. Kohse-Höinghaus, Combustion, chemistry, and carbon neutrality, *Chem. Rev.* 123 (2023) 5139–5219.
- [3] A. Omari, B. Heuser, S. Pischinger, C. Rüdinger, Potential of long-chain oxymethylene ether and oxymethylene ether-diesel blends for ultra-low emission engines, *Appl. Energy* 239 (2019) 1242–1249.
- [4] D. Pélerin, K. Gaukel, M. Härtl, E. Jacob, G. Wachtmeister, Potentials to simplify the engine system using the alternative diesel fuels oxymethylene ether OME1 and OME3–6 on a heavy-duty engine, *Fuel* 259 (2020) 116231.
- [5] N. Gaiser, T. Bierkandt, P. Obwald, et al., Oxidation of oxymethylene ether (OME0–5): An experimental systematic study by mass spectrometry and photoelectron photoion coincidence spectroscopy, *Fuel* 313 (2022) 122650.
- [6] N. Gaiser, H. Zhang, T. Bierkandt, et al., Investigation of the combustion chemistry in laminar, low-pressure oxymethylene ether flames (OME0–4), *Combust. Flame* 243 (2022) 112060.
- [7] H. Zhang, S. Schmitt, L. Ruwe, K. Kohse-Höinghaus, Inhibiting and promoting effects of NO on dimethyl ether and dimethoxymethane oxidation in a plug-flow reactor, *Combust. Flame* 224 (2021) 94–107.
- [8] M.U. Alzueta, J. Muro, R. Bilbao, P. Glarborg, Oxidation of dimethyl ether and its interaction with nitrogen oxides, *Isr. J. Chem.* 39 (1999) 73–86.
- [9] P. Dagaut, J. Luche, M. Cathonnet, The low temperature oxidation of DME and mutual sensitization of the oxidation of DME and nitric oxide: experimental and detailed kinetic modeling, *Combust. Sci. Technol.* 165 (2001) 61–84.
- [10] K.P. Shrestha, S. Eckart, A.M. Elbaz, et al., A comprehensive kinetic model for dimethyl ether and dimethoxymethane oxidation and NO_x interaction utilizing experimental laminar flame speed measurements at elevated pressure and temperature, *Combust. Flame* 218 (2020) 57–74.
- [11] M. Pelucchi, S. Schmitt, N. Gaiser, et al., On the influence of NO addition to dimethyl ether oxidation in a flow reactor, *Combust. Flame* 257 (2023) 112464.
- [12] X. He, M. Giese, L. Ruwe, A. Lucassen, K. Moshhammer, A detailed uncertainty analysis of EI-MBMS data from combustion experiments, *Combust. Flame* 243 (2022) 112012.
- [13] A. Stagni, S. Schmitt, M. Pelucchi, A. Frassoldati, K. Kohse-Höinghaus, T. Faravelli, Dimethyl ether oxidation analyzed in a given flow reactor: Experimental and modeling uncertainties, *Combust. Flame* 240 (2022) 111998.
- [14] P. Obwald, M. Köhler, An atmospheric pressure high-temperature laminar flow reactor for investigation of combustion and related gas phase reaction systems, *Rev. Sci. Instrum.* 86 (2015).
- [15] N. Gaiser, T. Bierkandt, P. Obwald, et al., Oxidation of linear and branched ethers: a comparative flow reactor study of OME2 and trimethoxymethane, *Proc. Combust. Inst.* 39 (2023) 685–693.
- [16] J.C. Biordi, Molecular beam mass spectrometry for studying the fundamental chemistry of flames, *Prog. Energy Combust. Sci.* 3 (1977) 151–173.
- [17] F. Herrmann, P. Obwald, K. Kohse-Höinghaus, Mass spectrometric investigation of the low-temperature dimethyl ether oxidation in an atmospheric pressure laminar flow reactor, *Proc. Combust. Inst.* 34 (2013) 771–778.
- [18] M. Schenk, L. Leon, K. Moshhammer, et al., Detailed mass spectrometric and modeling study of isomeric butene flames, *Combust. Flame* 160 (2013) 487–503.
- [19] A. Bodi, M. Johnson, T. Gerber, Z. Gengeliczki, B. Sztáray, T. Baer, Imaging photoelectron photoion coincidence spectroscopy with velocity focusing electron optics, *Rev. Sci. Instrum.* 80 (2009).
- [20] P. Obwald, P. Hemberger, T. Bierkandt, et al., In situ flame chemistry tracing by imaging photoelectron photoion coincidence spectroscopy, *Rev. Sci. Instrum.* (2014) 85.
- [21] B. Sztáray, K. Voronova, K.G. Torma, et al., CRF-PEPICO: Double velocity map imaging photoelectron photoion coincidence spectroscopy for reaction kinetics studies, *J. Chem. Phys.* (2017) 147.
- [22] T. Bierkandt, P. Obwald, N. Gaiser, et al., Observation of low-temperature chemistry products in laminar premixed low-pressure flames by molecular-beam mass spectrometry, *Int. J. Chem. Kinet.* 53 (2021) 1063–1081.
- [23] Y. Nunes, G. Martins, N.J. Mason, et al., Electronic state spectroscopy of methyl formate probed by high resolution VUV photoabsorption, He(i) photoelectron spectroscopy and ab initio calculations, *Phys. Chem. Chem. Phys.* 12 (2010) 15734–15743.
- [24] M. Hoener, T. Kasper, Nitrous acid in high-pressure oxidation of CH₄ doped with nitric oxide: challenges in the isomer-selective detection and quantification of an elusive intermediate, *Combust. Flame* 243 (2022) 112096.
- [25] D. Schröder, D. Sulzle, O. Dutuit, T. Baer, H. Schwarz, Further insight in the surprisingly complex unimolecular fragmentations of the methyl nitrite radical-cation, *J. Am. Chem. Soc.* 116 (1994) 6395–6400.
- [26] S. Jacobs, M. Döntgen, A.B. Alquaity, et al., Detailed kinetic modeling of dimethoxymethane. Part II: experimental and theoretical study of the kinetics and reaction mechanism, *Combust. Flame* 205 (2019) 522–533.
- [27] N. Li, W. Sun, S. Liu, et al., A comprehensive experimental and kinetic modeling study of dimethoxymethane combustion, *Combust. Flame* 233 (2021) 111583.
- [28] W. Sun, T. Tao, M. Lailliau, N. Hansen, B. Yang, P. Dagaut, Exploration of the oxidation chemistry of dimethoxymethane: Jet-stirred reactor experiments and kinetic modeling, *Combust. Flame* 193 (2018) 491–501.
- [29] F.H. Vermeire, H.-H. Carstensen, O. Herbinet, F. Battin-Leclerc, G.B. Marin, K. M. Van Geem, Experimental and modeling study of the pyrolysis and combustion of dimethoxymethane, *Combust. Flame* 190 (2018) 270–283.
- [30] A. Pegurri, T. Dinelli, L. Pratali Maffei, T. Faravelli, A. Stagni, Coupling chemical lumping to data-driven optimization for the kinetic modeling of dimethoxymethane (DMM) combustion, *Combust. Flame* 260 (2024) 113202.
- [31] Y. Song, L. Marrodán, N. Vin, et al., The sensitizing effects of NO₂ and NO on methane low temperature oxidation in a jet stirred reactor, *Proc. Combust. Inst.* 37 (2019) 667–675.
- [32] H. Minwegen, M. Döntgen, C. Hemken, R.D. Büttgen, K. Leonhard, K.A. Heufer, Experimental and theoretical investigations of methyl formate oxidation including hot β-scission, *Proc. Combust. Inst.* 37 (2019) 307–314.
- [33] J. Yang, D. Yan, Q. Mao, F. vom Lehn, H. Pitsch, L. Cai, A revised reaction kinetic mechanism for the oxidation of methyl formate, *Combust. Flame* 261 (2024) 113263.
- [34] E.E. Dames, A.S. Rosen, B.W. Weber, C.W. Gao, C.-J. Sung, W.H. Green, A detailed combined experimental and theoretical study on dimethyl ether/propane blended oxidation, *Combust. Flame* 168 (2016) 310–330.
- [35] Y. Zhang, S. Wang, Z. Zhang, L. Fu, H. Ning, H.Y. Zhao, Exploring the reaction kinetics of methyl formate + NO₂: implication for ignition behavior of methyl formate/NO₂ mixtures, *Phys. Chem. Chem. Phys.* 25 (2023) 32051–32061.
- [36] Y. Guan, X. Meng, X. Wang, R. Liu, H. Ma, J. Song, Theoretical mechanistic study on the reaction of the methoxymethyl radical with nitrogen dioxide, *J. Mol. Model.* 27 (2021) 18.
- [37] Y.L. Shang, J.C. Shi, L.M. Fang, Q.G. Feng, H.Y. Wang, S.N. Luo, Theoretical investigation on hydrogen abstraction by NO₂ from symmetric ethers (CH₃)₂xO (x = 1–4), *J. Phys. Chem. A* 122 (2018) 6829–6841.